TURBULENCE AND PRESSURE DROP BEHAVIORS AROUND SEMICIRCULAR RIBS IN A RECTANGULAR CHANNEL

by

Md. Julker NINE [a], ***Gyeong Hwan LEE*** [a], ***HanShik CHUNG*** [c], ***Myoungkuk JI*** [b], **and** ***Hyomin JEONG*** [c*]

[a] Department of Mechanical and Precision Engineering, Gyeongsang National University, Tongyeong, Gyeongnam, Korea
[b] Young Jin Forging Co., Ltd., Korea
[c] Department of Energy and Mechanical Engineering, Gyeongsang National University, Institute of Marine Industry, Tongyeong, Gyeongnam, Korea

Original scientific paper
DOI: 10.2298/TSCI111022142N

The article represents an experimental investigation on friction and turbulent flow characteristics of free airflow through a rectangular duct fitted with semicircular ribs of uniform height (e = 3.5 mm) on one principle wall. The aspect ratio of the rectangular duct was AR= 5 where the duct height was 30 mm. Four different rib pitches of 28 mm, 35 mm, 42 mm, and 49 mm were examined with constant rib height to hydraulic diameter ratio (e/Dh = 0.07) and constant rib height to channel height ratio (e/H = 0.116). The experimental results show some significant effects of pressure drop as well as turbulent characteristics at various configurations among different numbers of rib arrangements varying Reynolds number in the range of 15000 to 30000. Experimental results have been compared with numerical analysis and it can be seen a good agreement. The result explains the phenomena elaborately between two periodic ribs and enables to optimize the rib pitch ratio in terms of turbulence kinetic energy for maximum heat transfer.

Key words: *turbulence, friction factor, rectangular duct, semicircular rib*

Introduction

Periodic ribs are often employed in design of heat exchangers. Artificial roughness in the form of repeated ribs is considered as efficient method of augmentative heat transfer in a duct with fully developed fluid flow. Roughness with wire form and different shapes of ribs has been recommended by many researchers to enhance heat transfer in channel flow. The periodically arranged ribs in the channel interrupt hydrodynamic and thermal boundary layers. The flow around the ribs creates more vortices, circulations which enable to enhance thermal efficiency. The use of ribs not only works as a heat transfer enhancement rig but also creates huge pressure drop. The flow field depends on rib geometry and the rib arrangement inside the channel. Generally the rib angle, rib cross-section, rib height to channel height ratio and rib pitch influence in a great scale to the channel flow characteristics. That is why the optimization of rib

* Corresponding author; e-mail: hmjeong@gnu.ac.kr

shape and angle, rib pitch to rib height ratio and flow around rib geometry are essential parameters to get maximum efficiency from rib roughened heat exchanger.

This article focuses on pressure drop and turbulence characteristics to explain the phenomena occurred around semicircular ribs fitted in a rectangular channel as well as to optimize the rib pitch to rib height ratio in terms of turbulent kinetic energy. Several researches and inspections exist on pressure drop and heat transfer about rib roughened channel and still being developed the concept of different type roughness application to enhance heat transfer. The effect of rib pitch to height variation in a tube was first introduced by Webb *et al*. [1] and the result was formulated into a correlation. Most early researchers studied limited number of rib roughness configurations where the field demands to study more about optimal rib configurations for higher performance. Hanjalic and Launder [2] carried out detailed experiment of fully developed asymmetric flow in a plane channel. One of the surfaces was roughened by square silver steel ribs with a pitch to height ratio 10. Tanda [3] shows that 90° transverse ribs provided the lowest thermal performance and 60° parallel broken rib or 60° V-shaped broken ribs yielded a higher heat transfer augmentation than 45° parallel broken ribs. Han and Zhang [4] also found that 60° broken "V" ribs provide higher heat transfer at about 4.5 times than the smooth channel and the channel fabricated with continuous ribs. Chandra *et al*. [5] carried out measurements on heat transfer and pressure loss behaviors in a square channel with continuous rib fabricated on all four walls. They found the heat transfer augmentation increases with multiplying the number of ribbed wall. Huh *et al*. [6] shows the effect of rib spacing into the channel with 1:4 aspect ratio, where the rib pitch to rib height ratio were $P/e = 2.5$, 5, and 10 with a constant blockage ratio of $e/D_h = 0.078$. Mushatet [7] studied about the effect of a step height, the number of ribs and the rib thickness on the flow and they also analyzed thermal field of the system. The study shows that $P/\mathrm{e} = 10$ provides the best heat transfer performance. Hwang [8] reported that turbulent flow and convection heat transfer coefficients on variation of the radial component of hydrodynamic turbulence were dependent on rib size. Wilcox [9] applied k-ω turbulence model that considered the effect of surface roughness by changing only the surface boundary conditions from smooth to rough. The shear stress transport (SST) k-ω turbulence model presented by Menter [10] is a two-equation eddy-viscosity model. The SST formulation combines the better of two worlds. The use of a k-ω formulation in the inner parts of the boundary layer makes the model directly usable all the way down to the wall through the viscous sub-layer, hence the SST k-ω model can be used as a Low-Re turbulence model without any extra damping functions. Another numerical approach introduced by Durbin [11] for alternative eddy viscosity formulation, the v^2-f turbulence model uses an imaginary turbulent normal stress component, v'^2. This imaginary stress component is always normal to the closest wall and represents the turbulent velocity scale. Bakić *et al.* [12] investigated turbulent structures of flow around a sphere. The results of laser-Doppler measurements are compared with results obtained by large eddy simulation. In this paper also flow visualization around sphere has been done in the bigger wind tunnel and water channel for Reynolds numbers between 22,000 and 400,000.

In this article pressure drop and turbulent flow phenomena has been described elaborately and in much more comprehensive way around semicircular ribs. Experimental results are presented using four different rib configurations into turbulent channel flow under 15,000 to 30,000 Reynolds number. The principle aim of the experiment is to analyze the effect of semicircular ribs on friction and describe the flow characteristics as well as optimize rib pitch to rib height ratio for maximum turbulence kinetic energy recorded between two ribs. Two different turbulence models have been chosen because of their good capability especially for near wall treatment to make the study significant and comprehensive.

Experiment

The schematic diagram of the experimental apparatus is presented in fig. 1, where the details of the rib arrangement mounted on one principle wall of the rectangular duct is displayed. The measurement system of working fluid characteristics is also described.

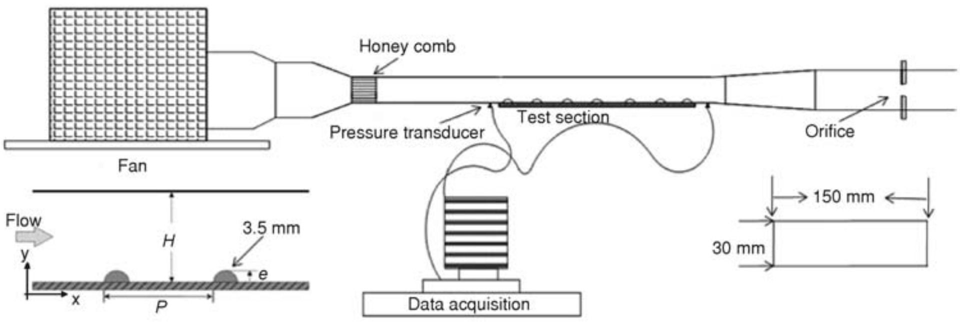

Figure 1. Schematic diagram of experimental set-up

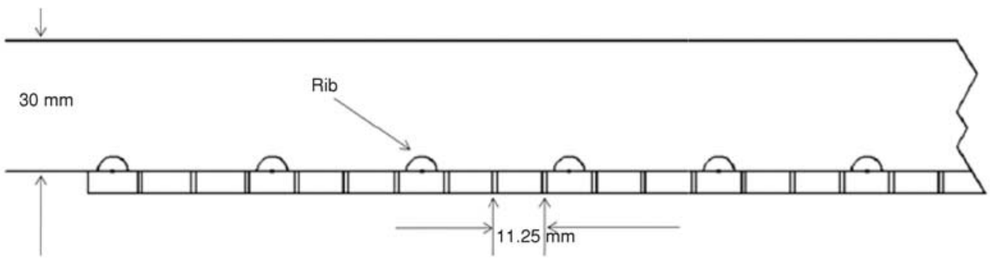

Figure 2. Small segment of ribbed test section with pressure taps

Experimental set-up

The rectangular duct is directly connected to a 0.5 kW low pressure blower. The channel geometry is characterized by the channel height (*H*) of 30 mm and 2500 mm axial length including 900 mm test section with the channel width of 150 mm. The ribbed wall is copper plate of 5 mm thickness on which several rib pitches of 28 mm and 35 mm, 42 mm, and 49 mm are used to find the best configuration. The uniform rib height (*e*) and rib thickness (*s*) are 3.5 mm and 7 mm, respectively. Air is tested fluid and the operating speed of the blower was varied by using a regulator to provide desired air velocity. Orifice meter is connected to the end off channel to measure the flow rate. Flow rate is calculated by measuring pressure differential between upstream and downstream of orifice. The diameter of orifice is 52.5 mm where the circular pipe holding orifice is used having same cross-sectional area of rectangular channel. Two static pressure taps are located at the bottom principle wall of channel to measure axial pressure drop across the test section to evaluate friction factor. One of pressure tap is 45 mm upstream from the leading edge of the test section and another is 45 mm downstream from the edge of test section.

Digital manometer is used for recording static pressure magnitude and hot wire anemometer is used to demonstrate near wall turbulence between two ribs.

Pressure drop measurement

The pressure drop investigation is performed at normal atmospheric condition. Static pressure taps are equipped at eighty one locations over all along the test section (shown in fig. 2) to measure adverse pressure gradient occurred by artificial roughness. Each of pressure tape is 11.25 mm apart from another along the centre of the channel having diameter of 1 mm. Short copper tubes were used in every pressure taps and glued with plastic rubber tubes which is connected to digital manometer to provide cross sectional average value of static pressure. During the data recording through one of those pressure taps, the others were kept closed using glue tape. In this way the whole 900 mm length of test sections static pressure were taken using digital micro manometer for both smooth and rib roughened surface. The difference of static pressure between two ribs shows the pressure gradient at different pitch ratio. Total pressure drop across entire test section is also demonstrated from two other pressure taps equipped at the inlet and outlet of test section.

Turbulence test

Specific location of approximately $29 < X/D_h < 32$ has been selected from the inlet of the duct to get the aerodynamic characteristics at various Reynolds numbers between two ribs. Straight I-type probe has been calibrated and used carefully to get the stream wise flow characteristics. FFT analysis of the hot wire signal shows that 512 samples per second can capture the high amplitude fluctuations in the flow around the ribs. Only one direction velocity fluctuation has been taken using I-type probe. In the direction of main stream, data has been taken between two ribs in a distance of 5 mm apart. But vertically data was taken from very near to bottom wall gradually step by step by the help of height gauge connected with hot wire anemometer stand, for 1st 1 mm from bottom wall was measured as 0.1 mm apart, 2nd 1 mm was taken as 0.2 mm apart, 3rd 1 mm was as 0.5 mm apart, in this way the 30 mm channel height data was taken very carefully using I-type probe with the help of digital height gauge. Turbulence kinetic energy has been measured only for axial direction (u) of velocity. For every single position between two ribs the mean velocity with time has been recorded. The fluctuation velocity along u component has been recorded as RMS value and finally turbulent intensity is derived by dividing RMS value by mean value. The average turbulent kinetic energy between two ribs are calculated using the data recorded moving the straight I-type probe in both of X- and Y-direction into the channel.

Bulk velocity (v_b) has been taken as arithmetic average velocity measured in both of axial and vertical direction at equally spaced by hot wire anemometer with the help of I-type probe over $29 < X/D_h < 32$ portion of test section. Specially fabricated the upper plate segment of rectangular channel was equally perforated exactly 1 cm apart and could be glided along stream wise direction by exchanging the position with another plate over the test section. By changing the position of plate one after another with small part perforated plate the whole test section has been measured for getting bulk velocity. While measuring velocity through a single hole the other holes were sealed perfectly from inside to out to be ensured that there is no leakage. After measuring bulk velocity this special setting has been removed and a single smooth part upper plate has been used for other measurement process to overcome unusual friction effect.

Numerical model

The ability to predict the characteristics of turbulent flow and heat transfer in a rectangular duct with artificial roughness ribs is investigated. Commercial computational fluid dynamics (CFD) software, FLUENT 6.3.26, was used to solve the equations.

SST k-ω model

The SST k-ω model combines the advantages of the k-ω and k-ε turbulence models. The k-ω model is well-suited for prediction in the vicinity of the wall, while the k- ε model is for the remaining area near the boundary region. The SST k-ω model is known to be fairly effective for better prediction of adverse pressure gradient and flow separation. The SST k-ω model has been designed to promote turbulence in the congestion zone of fluid flow.

In general, the role of turbulence models is to determine the turbulent viscosity correctly. The SST k - ω model can modify turbulent viscosity, calculating the impact of enhanced shear stress within the boundary layer resulting from continuing fluctuation of turbulent kinetic energy. This modification of turbulent viscosity improves the prediction of adverse pressure gradient and flow separation.

v2 -f model

The $v2$-f model is also a two-equation turbulence model similar to the standard k-ε turbulence model. The standard k-ε turbulence model is Reynolds stress approximate to the eddy viscosity model. Eddy viscosity is represented by k and ε, and is based on "$\nu_t \propto$ (turbulent velocity scale × turbulent length scale)". Kinetic eddy viscosity ν_t is calculated using a turbulent velocity scale (appearing from turbulent energy k) and turbulence length scale (appearing from specific dissipation rate ε of turbulent energy). But the k-ε turbulence model needs to use the wall function near the wall, which may result in inaccurate calculations, so the Low-Reynolds number k-ε model introduces an experiential damping function near the wall area that can calculate the viscous sub-layer region. However, the $\underline{v2}$-f model suggested by Durbin [11] uses an imaginary turbulent normal stress component, v'^2 instead of turbulent kinetic energy, k. This imaginary stress component is always normal to the closest wall and represents the turbulent velocity scale.

The transport equation for the normal-to-wall fluctuation velocity can be derived from the Reynolds stress equation with a linear pressure strain model and by simplifying the boundary layer. Because the pressure in a fluid flow is elliptic in nature, the correlation of fluctuating pressure and velocity gradient are also elliptic. The wall reflection (redistribution of normal stresses near the wall) is considered by means of elliptic relaxation.

Boundary condition and grid generation

Commercial CFD software, FLUENT 6.3.26, was used to solve the equations. The inlet and outlet boundary condition were set as mass flow rate using periodic condition. The mass flow obtained by experimental orifice meter are 0.031863 kg/s, 0.035731 kg/s, and 0.038973 kg/s which are converted into a 2-D flow rate 0.18763 kg/s, 0.21042 kg/s, and 0.22951 kg/s for numerical analysis. Main stream temperature is set 300 K.

The grid for the computations were consisted the number of 35,000-70,000 computational cells. Non-uniform structured grids are generated by Gambit shown in fig. 3 where the grids near the walls are fine enough. An exponential function was used to concentrate the fine

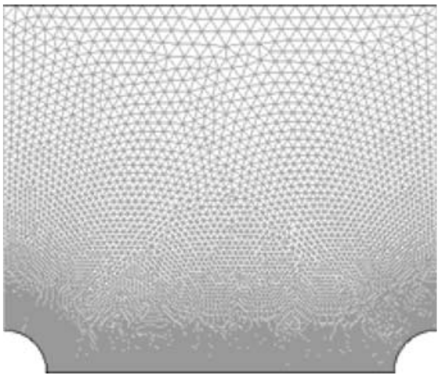

Figure 3. Numerical grid of the computational domain between two ribs for *P/e* = 8

mesh near the wall and rib surfaces to reserve the high-velocity gradients near the walls. The first grid point from the wall was carefully adjusted to be located in the linear region to ensure that non-dimensional wall distance y^+ was less than 1.0 [13].

The criterion for the convergence of the numerical solution was based on the normalized residuals of the equations which were summed for all cells in the computational domain. The solutions were regarded as converged when these normalized residuals were less than 10^{-6} for all flow variables and 10^{-9} for the energy equation.

In this study, to maintain better accuracy second order upwind difference scheme was applied though upwind difference scheme is used a lot as convection schemes difference. SIMPLE (semi-implicit method for pressure-linked equation) algorithm was used to link to velocity and pressure terms. In this treatment continuity equation is applied to find the correlation equations of pressure correction in the pressure field. The pressure and velocity can be obtained by solving the correlation equation in control volume.

Data reduction

Reynolds number is an independent parameter to optimize pitch ratio and comparing results with other characteristics. The Reynolds number (Re) based on the channel hydraulic diameter and bulk velocity is defined as:

$$\mathrm{Re} = \frac{V_\mathrm{b} D_\mathrm{h}}{\nu} = \frac{\rho V_\mathrm{b} D_\mathrm{h}}{\mu} \tag{1}$$

The dimensionless pressure drop characteristics are obtained by using Darcy-Weisbach equation which can be expressed by:

$$f = \frac{2}{\dfrac{L}{D_\mathrm{h}}} \frac{\Delta P}{\rho V_\mathrm{b}^2} \tag{2}$$

The range of Reynolds number conducted by the experiment is from 10,000 to 25,000. For the validation of smooth surface in this range for turbulent and fully developed flow Blasius correlation can be used found in open literature [14] as mentioned in eq. (3):

$$\begin{aligned} f_0 &= 0.316\,\mathrm{Re}^{-0.25}\ (\mathrm{Re} \le 20{,}000) \\ f_0 &= 0.184\,\mathrm{Re}^{-0.2}\ (\mathrm{Re} \ge 20{,}000) \end{aligned} \tag{3}$$

Turbulence kinetic energy has been measured only for u component of velocity.

Mean velocity (U_mean) is defined by:

$$U_\mathrm{mean} = \frac{\sum\limits_{i=1}^{N} u(t)}{N} \tag{4}$$

where N is the total number of data recorded in a period of time (i =1, 2, 3, … N)

Fluctuation velocity (U_{rms}) or rms value of u component is expressed in:

$$U_{\mathrm{rms}} = \sqrt{\overline{U}^2} = \sqrt{\frac{\sum_{i=1}^{N}[U_{\mathrm{mean}} - u(t)]^2}{N}} \tag{5}$$

Turbulent intensity (I) is:

$$I = \frac{U_{\mathrm{rms}}}{U_{\mathrm{mean}}} \cdot 100 \tag{6}$$

The kinetic energy of turbulence is the energy associated with turbulent eddies in a fluid flow. It can be defined as following equation for u velocity direction $k = \overline{U}^2/2$, for u component only.

Average turbulent kinetic energy is calculated by using:

$$k' = \frac{\sum_{j=1}^{n}}{n} \tag{7}$$

where n is the number of data taken from j number of position between two ribs to calculate average turbulent kinetic energy.

Average Nusselt number is defined as:

$$\mathrm{Nu} = \frac{hD_{\mathrm{h}}}{K} \tag{8}$$

where h is the convective heat transfer coefficient and K – the thermal conductivity of working fluid.

The enhancement factor (η) can be defined as a ratio of the heat transfer coefficient of an augmented surface to that of a smooth surface:

$$\eta = \frac{h}{h_0} = \frac{\mathrm{Nu}}{\mathrm{Nu}_0} \tag{9}$$

The estimation of experimental accuracy has been calculated following the method of uncertainty described by Kline and McClintock [15]. Digital manometer (Dwyer-Series 477) having tolerance ±0.5% at 16.6 °C to 27.6 °C has been used for static and differential pressure measurement. Calibration of I-type probe was done several times and it has been observed at low velocity the voltage fluctuation was little bit more comparing higher air velocity dragged by compressor. It has been found that the pressure fluctuation at a single point was ±2 Pa for repeated experiment where that of velocity was ±0.4 m/s. The overall uncertainty in friction factor and Reynolds number were ±8.54% and ±5.46%, respectively.

Result and discussion

Variation of dimensionless pressure drop with Reynolds number has been shown in fig. 4 in terms of friction factor. In this figure, the friction factor of smooth channel has been compared with Blasius correlation shown in eq. (3). The result from experiment shows good agreement with correlation with maximum deviation of ±8%. The axial pressure drop is affected by different rib pitch under turbulent flow. The channel encounters much pressure drop at lower rib pitch to rib height ratio. Friction factor reduces with increasing Reynolds number as well as

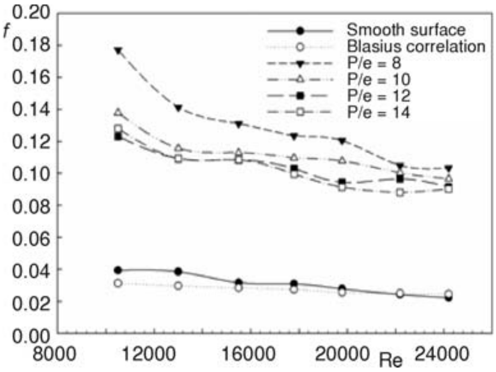

Figure 4. Friction factor for smooth and rib roughened surface

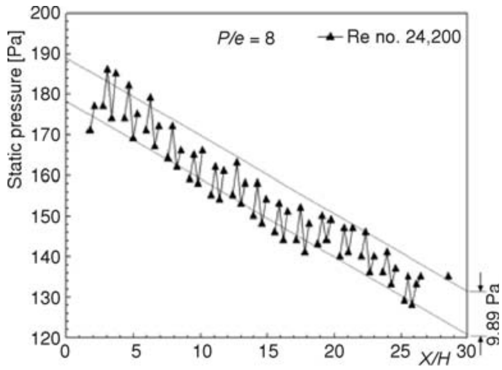

Figure 5. Static pressure of experimental data over test section for *P/e* = 8 at Re 24,200

with the rise of rib pitch to rib height ratio. It happens because channel contains more periodic rib at lower *P/e* ratio than fabricated by higher *P/e* ratio. So additional periodic ribs occur more flow resistance and reverse flow in the channel. The dissipation and reattachment of flow occurs between two ribs repeatedly which leads more friction loss and facilitates to enhance heat transfer.

The magnitude of adverse pressure gradient (fig. 5) has been acquired experimentally between two ribs by taking static pressure near the wall over whole test section. Adverse pressure gradient occurs when static pressure increases in the direction of flow. The reason of adverse pressure gradient is flow blockage by periodic ribs and it depends upon type of surface roughness. Rib height and rib pitch greatly affects pressure gradient. Reverse flow may occur because of high pressure gradient that makes flow separation. Experimentally evaluated pressure gradient value is 9.89 Pa for *P/e* = 8 at Reynolds number 24,200. The pressure drop in every single stage does not depend upon axial distance; the magnitude of pressure drop between two ribs is almost equal all along the test section for a specific Reynolds number.

The experimental pressure gradient value (shown in fig. 5) can be compared with numerical pressure gradient shown in fig. 6 where ν*2-f* model is found very close to the value obtained from experiment. It has been noticed that pressure drop across the length of 1 meter along whole test section depends on the pressure dropped at every single period of rib.

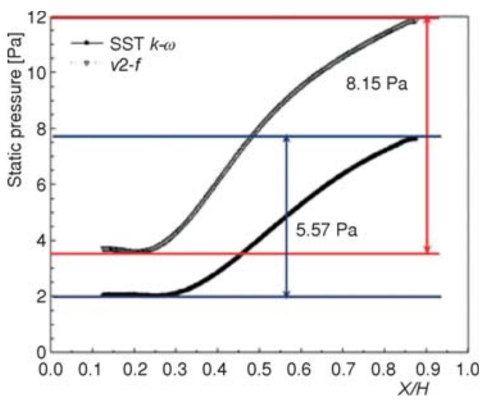

Figure 6. Static pressure predictions near the wall for *P/e* = 8 at Re 24,200

Figure 7 shows a mean velocity profile between two ribs at $P_x/e = 1.86$, $P_x/e = 4.71$, and $P_x/e = 7.45$ selected locations. The line probes of velocity profiles were selected between two ribs for *P/e* = 8, Re = 24,200 and mean velocity was measured to create velocity profile by using a hot-wire anemometer. The velocity profile resulting from CFD analysis was compared with experimental results at the same position. The ν2-*f* model result is closer to that of the experimental velocity profile.

In fig. 8, SST *k-ω* model shows the airflow distribution around semicircular rib for *P/e* = 8 at Reynolds number 24200. There happens a sudden expansion of fluid flow which makes a separation area at downstream the rib. After a big separation occurred behind the rib, there creates re-attachment of flow just in front of the next rib. The re-attachment and repeated circulation of flow influenced by the main stream and impinges on the wall as a result there creates a second small vortex. The result shows that the region "*Y* > 1.5*e*" is not influenced by the vortices or re-circulation zone.

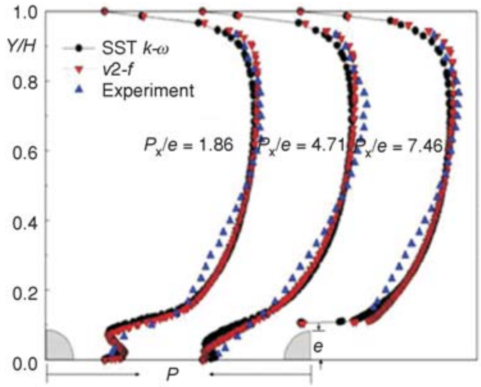

Figure 7. Mean velocity profile at various cross-stations for semicircular rib with *P/e* = 8 (for color image see journal web site**)**

Figure 9(a) shows line probes for measuring stream wise fluctuation component which indicates the position *Y/e* = 0.3 and 1.14. These two positions have been chosen to know near wall turbulent characteristics between two ribs and velocity fluctuation component at the flow separation zone. Stream wise fluctuation component comparing different pitch ratio at aforementioned position is displayed in fig. 9(b). At *Y/e* = 0.30 position, the fluctuation just after the rib gets pick, then gradually decreases until the middle of rib pitch and finally it again gets another pick just before the ribs. It happens periodically for all different rib pitch to rib height ratio (*P/e* = 8, 10, and 12). The position *Y/e* = 0.30 shows maximum fluctuation about 70% to 80% in the zone of re-circulation. So the fluctuation decay rate is independent of pitch ratio and it is amplified in second separation zone created just in front of the rib. But the rib height region at *Y/e* = 1.14 shows comparatively less fluctuation than near wall because the zone influenced by main stream does not get disturbed badly by flow separation. But more forwarding through this line increases turbulent intensity and again the intensity

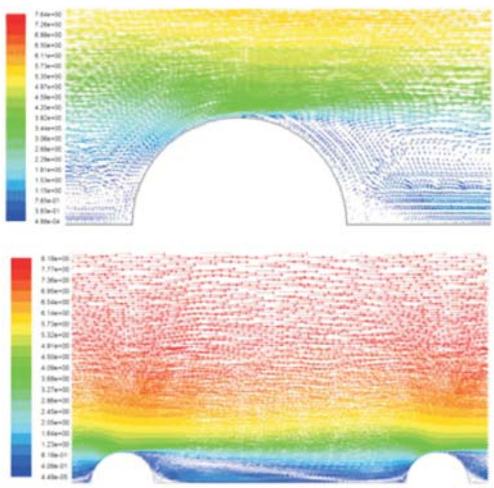

Figure 8. Velocity vectors (SST *k-ω* model) between two ribs with *P/e* = 8
(for color image see journal web site**)**

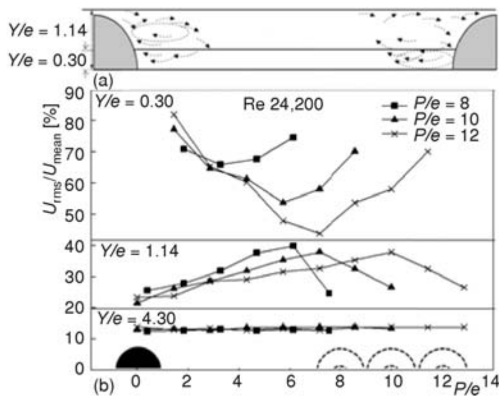

Figure 9. Steam wise turbulent intensity at Re 24,200; (a) line probes for measuring steam wise fluctuation component, (b) steam wise fluctuation component comparing different *P/e* ratio at *Y/e* = 0.30, 1.14, and 4.30

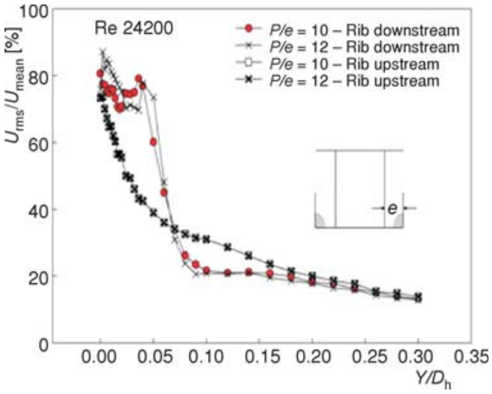

Figure 10. Comparison of vertically turbulent intensity between rib downstream and rib upstream

reduces when the probe line gets near the rib. Y/e = 4.30 position shows that the middle between two ribs is not roughly influenced by the re-circulation zone and for all P/e ratio similar characteristics can be founded.

Figure 10 exhibits stream wise turbulent intensity in vertical direction just before and after the ribs as shown in inset figure. The vertical measurement line has been chosen at two hotspots near the front and rear corners between two ribs. And these two corners can be introduced as primary and secondary re-circulation region. The figure shows two different patterns of measurement between downstream and upstream of the rib. Just behind the rib a large scale of measurement values having congestion together at high turbulence intensity (70% to 80%) until reaching the rib height position. It happens because of large scale re-circulation and flow separation. Sometimes large adverse pressure gradient causes back flow that leads the zone to more disorder flow. On the other hand after a big separation the flow impinges on the wall just before the rib and gets influenced by main stream though there creates a high pressure zone with little re-circulation. This primary part of re-circulation zone shows more regular measurement value comparing secondary re-circulation zone. So it is comprehensive to differentiate the performance of flow separation zone and re-attachment zone from this graph.

From fig. 11, it is obvious that P/e = 10 shows higher turbulent kinetic energy because the highest average turbulent intensity is derived from P/e = 10. The total average turbulent intensity depends upon the total area percentage captured by re-circulation and re-attachment zone between two ribs. The rib pitch to rib height ratio can be optimized by the total average turbulent kinetic energy produced by re-circulation and re-attachment zone between two ribs. Thermal enhancement has been numerically investigated and compared with experimental turbulent kinetic energy. The maximum thermal enhancement is achieved by P/e = 10 among all other rib pitch to rib height ratio (P/e). So it can be said that the heat transfer enhancement is dominated by turbulent transport between two ribs.

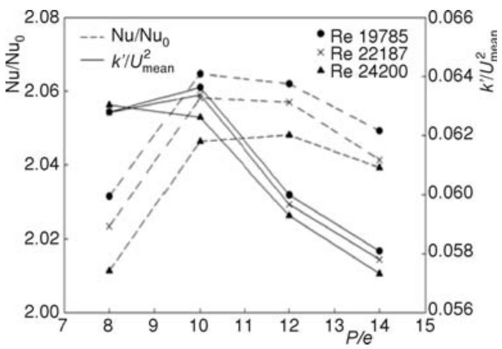

Figure 11. Left side – thermal enhancement calcualted from numerical analysis *vs. P/e*; right side – average turbulent kinetic energy calculated from experiment *vs. P/e*

Conclusions

The article analyzes friction and turbulent flow characteristics both in experimentally and numerically. For the convenience of analysis somewhere both results are compared. The prediction had a good similarity in case of pressure drop and aerodynamic analysis.

Friction factor is greatly influenced by rib pitch to rib height ratio where with increasing the number of P/e ratio decreases additional pressure loss at the same Reynolds number. Adverse pressure gradient due to surface friction around semicircular rib is well predicted by $v2$-f model, when compared with the experimental results. The pressure drop in every single stage does not depend upon axial distance; the magnitude of pressure drop between two ribs is almost equal all along the test section for a specific Reynolds number.

Turbulence phenomena at downstream and upstream of the rib are deferent in area of re-circulation and pressure difference. The re-circulation area in flow separation zone (secondary circulation) is larger than the re-attachment zone (primary vortex zone).

Stream wise velocity fluctuation gives higher value at re-circulation zone near bottom wall which is significant for heat transfer. The total average turbulent intensity depends upon the total area percentage captured by re-circulation and re-attachment zone between two ribs.

Overall pressure drop and turbulent intensity are two major factors influencing the heat transfer. $P/e = 10$ is found as optimal rib pitch to height ratio and described in terms of experimental turbulence kinetic energy and heat transfer enhancement. The heat transfer enhancement is dominated by total turbulent transport.

Acknowledgment

This research was supported by Basic Science Research Program through the National Research Foundation of Korea (NRF) funded by the Ministry of Education, Science and Technology (No. 2011-0021376).

Nomenclature

- AR – aspect ratio of rectangular channel
- D_h – hydraulic diameter of duct, [mm]
- e – rib height, [mm]
- f – friction factor
- H – channel height, [mm]
- h – convective heat transfer coefficient
- I – turbulent intensity, [%]
- K – thermal conductivity of working fluid, [$Wm^{-1}K^{-1}$]
- k – turbulent kinetic energy, [m^2s^{-2}]
- k' – average turbulent kinetic energy, [m^2s^{-2}]
- L – length of calculation domain, [mm]
- Nu – Nusselt number for rib roughened surface
- Nu_0 – Nusselt number for smooth surface
- P – rib pitch, [mm]
- P_x – axial distance between two ribs, [mm]
- P/e – rib pitch to rib height ratio
- ΔP – pressure drop, [Pa]
- Re – Reynolds number [$(V_b D_h/v)$]
- s – rib height, [m]
- t – time, [s]
- $u(t)$ – instantaneous velocity, [ms^{-1}]
- U_{mean} – mean velocity, [ms^{-1}]
- U_{rms} – stream wise velocity fluctuation, [mm]
- V_b – bulk velocity, [ms^{-1}]
- X – axial distance into channel, [m]

Greek symbols

- μ – dynamic viscosity, [$kgm^{-1}s^{-1}$]
- v – kinematic viscosity, [m^2s^{-1}]
- ρ – air density, [kgm^{-3}]

Reference

[1] Webb, R. L., *et al.*, Heat Transfer and Friction in Tubes with Repeated-Rib Roughness, *International Journal of Heat and Mass Transfer, 14* (1971), 4, pp. 601-617
[2] Hanjalic, K., Launder, B. E., Fully Developed Asymmetric Flow in a Plane Chanel, *Journal of Fluid Mechanics, 51* (1972), 2, pp. 301- 335
[3] Tanda, G., Heat Transfer in Rectangular Channels Transverse and V-Shaped Broken Ribs, *International Journal of Heat and Mass Transfer, 47* (2004), 2, pp. 229-243
[4] Han, J. C., Zhang, Y. M., High Performance Heat Transfer Duct with Parallel and V-Shaped Broken Rib, *International Journal of Heat and Mass Transfer, 35* (1992), 2, pp. 513-523
[5] Chandra, P. R., *et al.*, Heat Transfer and Friction Behavior in Rectangular Channel with Varying Number of Ribbed Walls, *International Journal of Heat and Mass Transfer, 46* (2003), 3, pp. 481-495

[6] Huh, M., *et al*., Effect of Rib Spacing on Heat Transfer in a Two-Pass Rectangular Channel (AR = 1:4) with a Sharp Entrance at High Rotation Numbers, ASME paper no. GT2008-50311, 2008
[7] Mushatet, K. S., Simulation of Turbulent Flow and Heat Transfer over a Backward -Facing Step with Ribs Turbulators, *Thermal Science, 15* (2011), 1, pp. 245-255
[8] Hwang, J. J., Heat Transfer-Friction Characteristic Comparison in Rectangular Ducts with Slit and Solid Ribs Mounted on the Wall, *ASME J. Heat Transfer, 120* (1998), 3, pp. 709-716
[9] Wilcox, D. C., *Turbulent Modeling for CFD*, DCW Industries Inc., 1994
[10] Menter, F. R., Zonal Two-Equation k-ω Turbulence Model for Aerodynamic Flow, AIAA Paper, pp. 1993-2906, 1993
[11] Durbin, P. A., A Reynolds Stress Model for Near-Wall Turbulence, *J. Fluid Mechanics, 249* (1993), April, pp. 456-498
[12] Bakić, V., *et al*., Experimental Investigation of Turbulent Structures of Flow Around a Sphere, *Thermal Science, 10* (2006), *2*, pp. 97-112
[13] ***, Fluent 6.3 User's Guide. Fluent Inc, 2003
[14] Incropera, F. P., DeWitt, D. P., Introduction to Heat Transfer, 2nd ed., John Wiley and Sons, New York, USA, 1990
[15] Kline, S. J., McClintock, F. A., Describing Uncertainties in Single Sample Experiments, *Mechanical Engineering, 57* (1953), pp. 3-8

Paper submitted: October 22, 2011
Paper revised: July 1, 2012
Paper accepted: July 11, 2012